



CHORUS

This is the accepted manuscript made available via CHORUS. The article has been published as:

Genetic Toggle Switch in the Absence of Cooperative Binding: Exact Results

Tommaso Biancalani and Michael Assaf

Phys. Rev. Lett. **115**, 208101 — Published 9 November 2015

DOI: [10.1103/PhysRevLett.115.208101](https://doi.org/10.1103/PhysRevLett.115.208101)

Genetic Toggle Switch in the Absence of Cooperative Binding: Exact Results

Tommaso Biancalani¹ and Michael Assaf²

¹*Department of Physics and Institute for Genomic Biology,
University of Illinois at Urbana-Champaign, Loomis Laboratory of Physics,
1110 West Green Street, Urbana, Illinois 61801-3080, USA*

²*Racah Institute of Physics, Hebrew University of Jerusalem, Jerusalem 91904, Israel*

We present an analytical treatment of a genetic switch model consisting of two mutually inhibiting genes operating without cooperative binding of the corresponding transcription factors. Previous studies have numerically shown that these systems can exhibit bimodal dynamics without possessing two stable fixed points at the deterministic level. We analytically show that bimodality is induced by the noise and find the critical repression strength that controls a transition between the bimodal and non-bimodal regimes. We also identify characteristic polynomial scaling laws of the mean switching time between bimodal states. These results, independent of the model under study, reveal essential differences between these systems and systems with cooperative binding, where there is no critical threshold for bimodality and the mean switching time scales exponentially with the system size.

PACS numbers: 87.18.Cf, 87.16.-b, 05.40.-a, 02.50.Ey

Gene expression in living cells is regulated by transcription factors that bind to specific DNA sequences thereby promoting or repressing transcription of genes. This mechanism allows for a “digital” response: when a cell has to make a decision, between expressing a certain protein, A , or another, B , a biochemical regulatory network leads the system to a state either dominated by A , or B . Such behavior is called bimodal. An example of such decision-making circuits is given by the genetic toggle switch in which two transcription factors mutually repress each other [1, 2]. This and other genetic switches allow cells to switch between distinct phenotypic states and determine the cell’s fate, in response to environmental stimuli and/or internal signals [3–6].

Genetic switches are found to exhibit distinct behaviors according to whether or not there is cooperative binding (CB) of transcription factors (see *e.g.* [7] in the context of positive feedback). If CB is in play, more than a single transcription factor molecule can bind to the DNA sequence, and the binding probability depends on whether there are molecules already bound to the sequence. CB is a driver of bimodality and was previously thought to be a necessary condition for a bimodal behavior [8–11]. This is since when CB is present in the rate equations, there are (at least) two stable fixed points corresponding to states rich in each type of transcription factors; in contrast, the absence of CB yields a single stable fixed point where the two transcription factors coexist.

Yet, in recent years, it has been shown in different models theoretically [12–14], and experimentally [7], that bimodality can emerge even without having bistability at the deterministic level. In [7], bimodality has been reported in a synthetic budding yeast system, which concluded that the bimodal behavior is induced by demographic noise. In Refs. [13, 14], the authors have numerically shown that a genetic toggle switch can exhibit a bimodal behavior due to demographic noise, even in

the absence of CB. To this end, in Ref. [15] the exclusive switch model (ESM) was analytically studied via the probability generating function. Yet, their analysis, valid only in limiting cases, cannot uncover how demographic noise gives rise to bimodal dynamics. Thus, the mechanism of noise-induced bimodality in such systems without CB remains unclear.

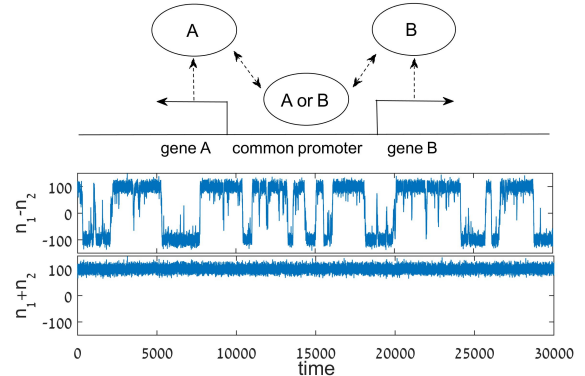


FIG. 1. Top: a schematic plot of the ESM [14]. The repressors A and B cannot be bound simultaneously due to overlap between their promoter sites. Middle and bottom: the difference and sum of the copy numbers of A and B obtained from stochastic simulations [16], with $\alpha = 0.01$, $k = 10$ and $g = 1$.

In this Letter we present an analytical treatment of the ESM, see Fig. 1, which is found, *e.g.*, as a coarse-grained description of the lysis-lysogeny switch of phage λ [1, 2]. We begin by analyzing the case of equal degradation rates of the transcription factors. We show that bimodality is driven by multiplicative noise, thus the bimodal states correspond to states for which the noise in the system vanishes. We further find a transition between the bimodal and non-bimodal regimes controlled by the noise strength, and identify the onset of bimodality as function of the repressor strength. Finally, we show that

the mean switching time (MST) from a state rich in A to a state rich in B scales polynomially in the system size, unlike typically found in bistable systems. These claims are then generalized to the case of different degradation rates using an adiabatic approximation. Finally, we show that our results hold for other models displaying noise-induced bimodality such as the general toggle switch [13, 14]. Our analysis is also available in the Supplemental Material (SM) and *Mathematica* files.

The genetic toggle switch models mutual inhibition and degradation of transcription factors. In the case of ESM, there is an overlap between the promoters of A and B preventing simultaneous occupation of the two [10, 13], see Fig. 1. Thus, at the deterministic level, the dynamics of the free proteins A and B , and the bound proteins, r_A and r_B , satisfy the following set of equations [14]

$$\begin{aligned}\dot{n}_1 &= g_A(1 - r_B) - d_A n_1 - \kappa_0 n_1(1 - r_A - r_B) + \kappa_1 r_A \\ \dot{n}_2 &= g_B(1 - r_A) - d_B n_2 - \kappa_0 n_2(1 - r_A - r_B) + \kappa_1 r_B \\ \dot{r}_A &= \kappa_0 n_1(1 - r_A - r_B) - \kappa_1 r_A \\ \dot{r}_B &= \kappa_0 n_2(1 - r_A - r_B) - \kappa_1 r_B.\end{aligned}\quad (1)$$

Here n_1 and n_2 denote the copy-numbers of proteins A and B , respectively. Also, g_A and g_B are the maximal production rates of proteins A and B , and d_A and d_B , the corresponding degradation rates. In addition, the bound repressors r_A and r_B , $0 \leq r_A, r_B \leq 1$, are bound A and B proteins that monitor the production of B and A , respectively, κ_0 denotes the binding rate of proteins to the promoter while κ_1 is the dissociation rate.

For simplicity we will henceforth assume $g_A = g_B = g$. In the limit of $d_A, d_B \ll \kappa_1$, the relaxation of the bound proteins is fast compared to that of the free proteins. As a result, in this limit, one can adiabatically eliminate the fast variables r_A and r_B and arrive at a set of two Michaelis-Menten-like rate equations for n_1 and n_2 [14]:

$$\dot{n}_1 = f_1(n_1, n_2) - \alpha_1 n_1, \quad \dot{n}_2 = f_2(n_1, n_2) - \alpha_2 n_2, \quad (2)$$

where $f_i(n_1, n_2) = (1 + kn_i)/(1 + kn_1 + kn_2)$. Here we have defined the dimensionless repression strength $k = \kappa_0/\kappa_1$ as the ratio of the binding and unbinding rates, $\alpha_1 = d_A/g$ and $\alpha_2 = d_B/g$ are the rescaled degradation rates of A and B , and we have rescaled time $t \rightarrow gt$. We will further assume that $\alpha_1 = \alpha_2 \equiv \alpha$, which will be generalized later on.

In this paper we focus on the strong repression limit, $kn_i \gg 1$ ($i = 1, 2$) [14], which is found (*e.g.*) in a bacterial genetic switch [8]. Since at the fixed point of system (2) $n_i \sim \alpha^{-1}$, see below, the strong repression limit becomes $\varepsilon \equiv \alpha/k \ll 1$, and one can naturally define the concentrations of A and B by $x_1 = \alpha n_1$, $x_2 = \alpha n_2$, respectively. The scaling of the fixed points allows us to introduce the effective system size α^{-1} . Yet, while α^{-1} is proportional to the physical system size N originating from system (1), they are not identical. In the SM we discuss in detail the relationship between our rescaled parameters

and the physical system size, and we also comment about the biological relevance of our approximations. Finally, note that at the fixed point, $n_1^* = n_2^* \simeq (1 + \varepsilon)/(2\alpha)$, see SM, indicating that, in the deterministic limit, the system converges into an equal state of A 's and B 's.

To account for demographic stochasticity ignored by Eqs. (2), we can write down the corresponding master equation for the probability P_{n_1, n_2} to find n_1 and n_2 molecules of type A and B , respectively. Defining the step operator $E_n^\pm F(n) = F(n \pm 1)$, we have (see SM):

$$\begin{aligned}\dot{P}_{n_1, n_2} &= [(E_{n_1}^- - 1)f_1(n_1, n_2) + (E_{n_2}^- - 1)f_2(n_1, n_2) \\ &\quad + \alpha_1(E_{n_1}^+ - 1)n_1 + \alpha_2(E_{n_2}^+ - 1)n_2] P_{n_1, n_2}.\end{aligned}\quad (3)$$

Using the Gillespie algorithm [16], stochastic system (3) is simulated and shown to exhibit bimodality in some range of parameters (middle panel in Fig. 1), in sharp contrast with the deterministic dynamics (2) [13, 14].

To this end, we introduce two auxiliary variables: the total concentration, $w = x_1 + x_2$, and the (adimensional) concentration difference $u = (x_1 - x_2)/(x_1 + x_2)$. Note that $u \approx \pm 1$ when the system is rich in one type of transcription factor, whereas $u \approx 0$ at the deterministic fixed point. For strong repression, $\varepsilon \ll 1$, the joint stationary probability density function (PDF), $\mathcal{P}_s(u, w)$, decouples and satisfies $\mathcal{P}_s(u, w) = P_s(u)R_s(w)$ (see SM). Here

$$R_s(w) = (2\pi\alpha)^{-1/2} e^{-\frac{[w - (1+\varepsilon)]^2}{2\alpha}}, \quad (4)$$

indicating that the sum of A 's and B 's, represented by w , is approximately conserved. To find $P_s(u)$, we consider its Langevin equation (see SM)

$$du/d\tilde{t} = -u + \sqrt{k}\sqrt{1-u^2}\eta(\tilde{t}), \quad (5)$$

where $\tilde{t} = 2g\epsilon\alpha t = 2g\alpha^2 t/k$, t is the physical time used in (1), and $\eta(t)$ denotes normalized Gaussian white noise.

Equation (5) captures the stochastic dynamics of the system. It has already been treated in previous works [17, 18], and suggests an explanation for the occurrence of bimodality in the genetic toggle switch. The deterministic drag, $-u$, attracts the system to the stable fixed point, $u^* = 0$, but since at this state the noise has maximum strength, \sqrt{k} , the value of u is driven away, toward those states at which the noise vanishes, $u = \pm 1$. These are the bimodal states and replace the deterministic fixed points in the CB case. How does this result depend on the repressor strength k ? Our previous argument has assumed that the noise strength at fixed point is large enough to oppose the deterministic drag. Yet, taking $k \rightarrow 0$, yields $\dot{u} = -u$, and thus $u(t) \rightarrow 0$ as $t \rightarrow \infty$. We can thus expect that for small k 's, the system fluctuates around $u = 0$ without exhibiting bimodality. This transition from unimodality to bimodality is elucidated by the stationary PDF, $P_s(u)$, of Eq. (5) [19]. We find

$$P_s(u) = \mathcal{N}(1 - u^2)^{(1-k)/k}, \quad (6)$$

where $\mathcal{N} = \Gamma(k^{-1} + 1/2) / [\sqrt{\pi} \Gamma(k^{-1})]$ is a normalization constant such that $\int_{-1}^1 P_s(u) du = 1$. Defining the critical repressor strength, $k_C = 1$ (where the PDF concavity is changed), we find two distinct regimes: non bimodal, $k < k_C$, where the system displays Gaussian fluctuations around the fixed point $u^* = 0$, and bimodal, $k > k_C$, where the system exhibits bimodality and switches between the states $u = \pm 1$. In Fig. 2, Eq. (6) excellently agrees with simulations for different values of k . Finally, that PDF (6) satisfies $|P_s(u + \alpha) - P_s(u)| \ll P_s(u)$, at $u \in (-1, 1)$, validates a-posteriori the Fokker-Planck approximation, see SM, to the master equation (3) [20, 21].

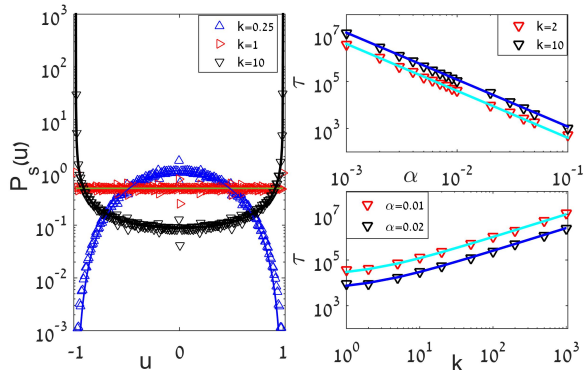


FIG. 2. Left panel: The PDF $P_s(u)$ for different values of k . For $k > 1$, a bimodal PDF appears, for $k = 1$ the PDF is flat and, for $k < 1$, unimodal with a peak on $u = 0$. Solid lines are given by Eq. (6) while markers are obtained by simulations [16], with $\alpha = 0.01$. Right panels: The MST as a function of α (upper right panel) and k (lower right panel) for $g = 1$. Each marker is obtained by averaging 200 numerical realizations [16], whereas solid lines are given by Eq. (7).

Equation (5) also allows calculating the MST between the bimodal states [17, 18]. In the bimodal regime, the MST τ is the mean time it takes the system to go from a state rich in one transcription factor, say $u = 1$, to a state rich in the other, $u = -1$, or vice versa. As shown in [17, 18], for $k \gg 1$, the MST of Eq. (5) reads

$$\tau \simeq (k + 2)/(g\alpha^2), \quad (7)$$

where we have restored the original time units used in (1). This result (checked against simulations in Fig. 2) depends polynomially on the effective system size α^{-1} , in contrast with the usually found exponential dependence of the mean escape time in bistable switches, see *e.g.* Refs. [22–26]. Hence, the absence of CB allows for much more frequent switching between different phenotypic states, which can be beneficial, *e.g.*, in cases of severe stress [27].

The previous results can be generalized to the case of different degradation rates, which can be analyzed using an adiabatic elimination of the w variable [19, 28, 29]. A similar treatment can also be used to investigate the case

of different repression strengths $k_1 \neq k_2$. Yet, as can be checked, for $\varepsilon \ll 1$ the effect of uneven k 's on the PDF and MST is much weaker than the effect of uneven α 's.

We again consider Eqs. (2) assuming, without loss of generality, $\alpha_2 < \alpha_1$, and denote $\alpha_1 \equiv \alpha$ and $\alpha_2 \equiv \delta\alpha$, where $\delta \in (0, 1]$. Defining $u = (x_1 - x_2)/(x_1 + x_2)$ and $w = x_1 + x_2$, where $x_1 = \alpha n_1$ and $x_2 = \alpha n_2$ are the concentrations, the stationary PDF, $Q_s(u)$, of finding concentration u , reads (see SM for details)

$$Q_s(u) = \mathcal{Z} P_s(u) (1 + u + \delta - u\delta)^{-1 - \frac{2}{\alpha(1+\delta)}} \times \exp\left(\frac{1}{k} \left(\frac{1-\delta}{1+\delta}\right) \left[2u + \ln\left(\frac{1-u}{1+u}\right)\right]\right), \quad (8)$$

where $P_s(u)$ is given by Eq. (6), and \mathcal{Z} is a normalization factor such that $\int_{-1}^1 Q_s(u) du = 1$. Our theory [Eq. (8)] excellently agrees with simulations, see Fig. 3.

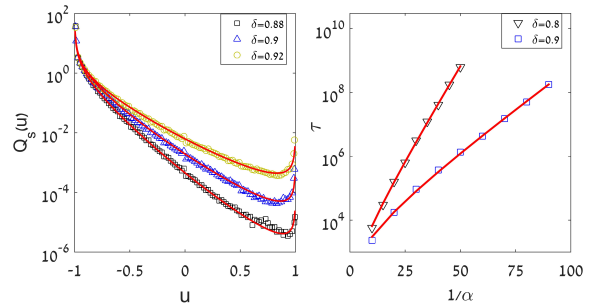


FIG. 3. Left panel: $Q_s(u)$ [Eq. (8)] (solid lines) is compared for different values of δ against simulations [16] (symbols). Here $k = 5$ and $\alpha = 0.01$. Right panel: MST τ versus $1/\alpha$, for $k = 50$ and $g = 1$. Each marker is obtained by averaging 200 numerical realizations, while the solid lines are given by Eq. (9) with $A = 50$ for $\delta = 0.8$ and $A = 100$ for $\delta = 0.9$.

The PDF (8) is a tilted version of PDF (6); indeed, the former reduces to the latter for $\delta = 1$. Since we have chosen $\delta < 1$, we find that the system resides most of the time at the metastable mode of $u = -1$ and occasionally jumps to the transiently metastable mode of $u = 1$ (the opposite would occur for $\delta > 1$). Similarly as for the case of $\delta = 1$, by decreasing k there exists a transition from a state rich in one type of transcription factor to a state where both types coexist, although not equally. Again, this is determined by a critical repressor strength k_C , satisfying $k_C = 2/(1 + \delta)$, see SM. For $k > k_C$, both $u = 1$ and $u = -1$ are noise-induced metastable states, although the system is biased toward $u = -1$ as the degradation rate of the corresponding protein (of type B) is smaller. In contrast, as k is decreased below k_C , the PDF flips, and peaks at $u^* = -1 + \mathcal{O}(\varepsilon)$, see SM.

Since the MST τ from $u = -1$ to $u = 1$ turns out to depend exponentially on the effective system size α^{-1} (see below), given Eq. (8), τ satisfies in the leading order $\tau \sim Q_s(-1) / \min[Q_s(u)]$ [22, 30]. Here, the minimum of $Q_s(u)$ is obtained in the close vicinity of $u = 1$, satisfying

$u_m \simeq 1 - 2\varepsilon(k/k_C - 1)/(1 - \delta) \simeq 1$. As $Q_s(u)$ diverges at $u = -1$, we thus compute the limit $\lim_{\alpha \rightarrow 0} Q_s(-1 + a)/Q_s(u_m)$ and find, in the leading order of $\varepsilon \ll 1$

$$\tau \simeq \frac{\mathcal{A}}{g\alpha} \exp \left[\frac{2}{\alpha(1 + \delta)} \ln \frac{1}{\delta} \right]. \quad (9)$$

Here $\mathcal{A} = \mathcal{A}(k, \delta)$ is an unknown prefactor, and we have restored the physical time units. Equation (9) agrees well with simulations, see Fig. 3, and in contrast to Eq. (7), depends exponentially on the effective system size.

Finally, we can use the analysis above for other models that exhibit noise-induced bimodality such as the general toggle switch, described by Eqs. (2) with

$$f_i(n_1, n_2) = [1 + (kn_j)^h]^{-1}, \quad i \neq j = 1, 2 \quad (10)$$

where the Hill coefficient is $h = 1$ [14]. In principle, the analysis can be done in the same manner as for the ESM. Yet, the task is slightly more difficult since the Langevin equation for $w = x_1 + x_2$ does not yield a Gaussian PDF for $R_s(w)$, which makes the equation for u less tractable. Nonetheless, we have numerically found the onset of bimodality to be at $k > k_C = 1$ and that the MST behaves similarly to the ESM, see Fig. 4. In sharp contrast, the genetic toggle switch model *with* CB, for which $f_i(n_1, n_2)$ are given by Eq. (10) with Hill coefficient $h \geq 2$, displays (at least) two stable fixed points. In this case there is no threshold for bimodality when $\varepsilon \ll 1$, and one expects an exponential dependence of the MST on the system's size [31]. In Fig. 4 we compare the MSTs and PDFs of several models with and without CB. Our simulations indicate that the MST in the case of CB with $h \geq 2$ yield a stretched-exponential dependence of the MST on the system's size. This is a nontrivial result and requires a further study. While this is beyond the scope of this paper, we believe the formalism we have developed can be used to study toggle switch models with CB as well, as long as we are in the strong repression limit.

We have presented an analytical treatment of the ESM demonstrating a bimodal behavior in the absence of two stable fixed points at the deterministic level. Bimodality is induced by multiplicative noise: the noise strength vanishes at the bimodal states whereas it is maximal at the single stable fixed point. This phenomenon, which has attracted much interest in various fields [17, 32–36], is linked here to previous numerical [13, 14] and experimental [8] findings on the genetic toggle switch.

We have shown that bimodal behavior ceases to occur if the noise strength in the system, controlled by the repression strength k , is reduced below a critical threshold. This transition, absent in bistable systems, is similar to that found in other noise-induced bimodal systems [17, 32, 37]. Moreover, we have shown here that the MST between bimodal states exhibits a polynomial, rather than exponential, scaling on the system size. In

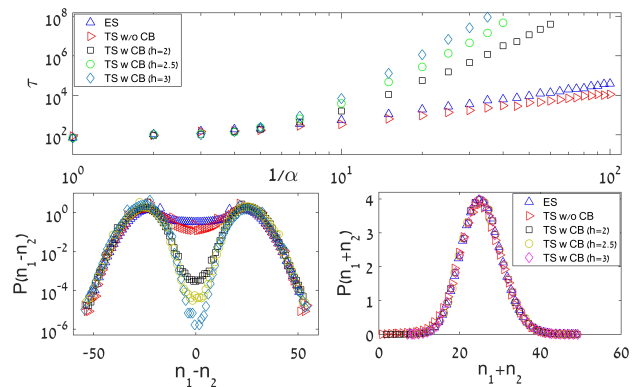


FIG. 4. (Top) MSTs for five different models: ESM, general toggle switch (TS) without (w/o) CB, and TS with (w) CB with $h = 2, 2.5, 3$, for $k = 1.5$. Each point is obtained by averaging 200 realizations. (Bottom) PDFs of the difference and sum of the copy numbers n_1 and n_2 , for $k = 5$ and $\alpha = 0.04$. While $P(n_1 + n_2)$ almost coincides for all models, the “potential barrier” for switching given by $\max[P(n_1 - n_2)] - \min[P(n_1 - n_2)]$, is much shallower for models without CB.

genetic toggle switches, the noise is controlled by the repression strength k , suggesting that bimodality can be achieved or lost by biological fine tuning of reaction rates.

We would like to thank Ofer Biham for valuable discussions. This work was supported by Grant No. 300/14 of the Israel Science Foundation. T.B. acknowledges partial support from the National Aeronautics and Space Administration through the NASA Astrobiology Institute under Cooperative Agreement No. NNA13AA91A issued through the Science Mission Directorate.

-
- [1] M. Ptashne, Cell and Blackwell Scientific, Cambridge, MA (1992).
 - [2] I. Golding, Annual review of biophysics **40**, 63 (2011).
 - [3] M. B. Elowitz, A. J. Levine, E. D. Siggia, and P. S. Swain, Science **297**, 1183 (2002).
 - [4] M. Thattai and A. Van Oudenaarden, Proc. Natl. Acad. Sci. U.S.A. **98**, 8614 (2001).
 - [5] J. Hasty, J. Pradines, M. Dolnik, and J. J. Collins, Proc. Natl. Acad. Sci. U.S.A. **97**, 2075 (2000).
 - [6] H. H. McAdams and A. Arkin, Proc. Natl. Acad. Sci. U.S.A. **94**, 814 (1997).
 - [7] T.-L. To and N. Maheshri, Science **327**, 1142 (2010).
 - [8] T. S. Gardner, C. R. Cantor, and J. J. Collins, Nature **403**, 339 (2000).
 - [9] P. B. Warren and P. R. ten Wolde, J. Phys. Chem. B **109**, 6812 (2005).
 - [10] R. J. Allen, P. B. Warren, and P. R. Ten Wolde, Phys. Rev. Lett. **94**, 018104 (2005).
 - [11] D. Schultz, A. M. Walczak, J. N. Onuchic, and P. G. Wolynes, Proc. Natl. Acad. Sci. U.S.A. **105**, 19165 (2008).
 - [12] M. Samoilov, S. Plyasunov, and A. P. Arkin, Proc. Natl. Acad. Sci. U.S.A. **102**, 2310 (2005).

- [13] A. Lipshtat, A. Loinger, N. Q. Balaban, and O. Biham, Phys. Rev. Lett. **96**, 188101 (2006).
- [14] A. Loinger, A. Lipshtat, N. Q. Balaban, and O. Biham, Phys. Rev. E **75**, 021904 (2007).
- [15] J. Venegas-Ortiz and M. R. Evans, Journal of Physics A: Mathematical and Theoretical **44**, 355001 (2011).
- [16] D. T. Gillespie, J. Phys. Chem. **81**, 2340 (1977).
- [17] T. Biancalani, L. Dyson, and A. J. McKane, Phys. Rev. Lett. **112**, 038101 (2014).
- [18] T. Biancalani, L. Dyson, and A. J. McKane, J. Stat. Mech. **2015**, P01013 (2015).
- [19] C. W. Gardiner, *Handbook of Stochastic Methods for Physics, Chemistry and the Natural Sciences*, 4th ed. (Springer, New York, 2009).
- [20] C. R. Doering, K. V. Sargsyan, and L. M. Sander, Multiscale Modeling & Simulation **3**, 283 (2005).
- [21] M. Assaf and B. Meerson, Phys. Rev. E **75**, 031122 (2007).
- [22] M. Dykman, E. Mori, J. Ross, and P. Hunt, The Journal of chemical physics **100**, 5735 (1994).
- [23] C. Escudero and A. Kamenev, Phys. Rev. E **79**, 041149 (2009).
- [24] M. Assaf and B. Meerson, Phys. Rev. E **81**, 021116 (2010).
- [25] M. Assaf, E. Roberts, and Z. Luthey-Schulten, Phys. Rev. Lett. **106**, 248102 (2011).
- [26] J. M. Newby, J. Phys. A **48**, 185001 (2015).
- [27] N. Q. Balaban, J. Merrin, R. Chait, L. Kowalik, and S. Leibler, Science **305**, 1622 (2004).
- [28] G. W. Constable and A. J. McKane, Phys. Rev. E **89**, 032141 (2014).
- [29] N. G. van Kampen, *Stochastic Processes in Physics and Chemistry*, 3rd ed. (Elsevier Science, Amsterdam, 2007).
- [30] M. Assaf and B. Meerson, Phys. Rev. Lett. **97**, 200602 (2006).
- [31] J. M. Newby, Phys. Bio. **9**, 026002 (2012).
- [32] Y. Togashi and K. Kaneko, Phys. Rev. Lett. **86**, 2459 (2001).
- [33] C. R. Doering, Phys. Rev. A **34**, 2564 (1986).
- [34] M. N. Artyomov, J. Das, M. Kardar, and A. K. Chakraborty, Proc. Natl. Acad. Sci. U.S.A. **104**, 18958 (2007).
- [35] J. Ohkubo, N. Shnerb, and D. Kessler, J. Phys. Soc. Jpn. **77**, 044002 (2007).
- [36] D. Remondini, E. Giampieri, A. Bazzani, G. Castellani, and A. Maritan, Physica A **392**, 336 (2013).
- [37] D. Russell and R. Blythe, Phys. Rev. Lett. **106**, 165702 (2011).